

Supporting Information

D-A- π -A organic dyes with tailored green light absorption for potential application in greenhouse-integrated Dye-Sensitized Solar Cells

Alessio Dessì,^{a,*} Dimitris A. Chalkias,^b Stefania Bilancia,^c Adalgisa Sinicropi,^{a,c,d} Massimo Calamante,^{a,e}
Alessandro Mordini,^{a,e} Aggeliki Karavioti,^b Elias Stathatos,^{b,*} Lorenzo Zani,^a Gianna Reginato^{a,*}

^a Institute of Chemistry of Organometallic Compounds (CNR-ICCOM), Via Madonna del Piano 10, I-50019 Sesto Fiorentino, Italy; ^b Nanotechnology & Advanced Materials Laboratory, Department of Electrical and Computer Engineering, University of Peloponnese, GR-26334 Patras, Greece; ^c Department of Biotechnology, Chemistry and Pharmacy, University of Siena, Via A. Moro 2, I-53100, Siena, Italy; ^d CSGI, Consorzio per lo Sviluppo dei Sistemi a Grande Interfase, Sesto Fiorentino I-50019, Italy; ^e Department of Chemistry "U. Schiff", University of Florence, Via della Lastruccia 13, I-50019 Sesto Fiorentino, Italy.

Table of Contents

1. Computational details.....	S2
2. Synthesis of the new dyes.....	S3
2.1. Materials and methods.....	S3
2.2. Synthetic procedures.....	S3
2.3. Additional details on the double direct arylation of compound 7	S6
3. Spectroscopic and electrochemical measurements.....	S7
4. Dye-Sensitized Solar Cells Fabrication and Characterization.....	S7
4.1. Materials.....	S7
4.2. Fabrication of the dye-sensitized solar cells.....	S8
4.3. Characterization of the dye-sensitized solar cells.....	S9
5. Additional figures.....	S10
6. Copies of the NMR spectra of compounds 3 , 4 , 6 , 8 and BTD-DTP1-3	S15
7. References.....	S29

1. Computational details

Ground state geometry optimization was carried out in vacuo using the B3LYP functional^{1,2} and the standard 6-31G* basis set for all atoms. The absorption maximum (λ^a_{\max}), vertical excitation energy (E_{exc}), and oscillator strength (f) in solution were calculated on the minimum structures via time-dependent DFT (TD-DFT) at the CAM-B3LYP³/6-311G(d,p) level of theory. Solvent effects have been included by using the polarizable continuum model (PCM).⁴

Geometry optimizations of the dyes on TiO₂ were carried out using a Ti₁₆O₃₂ model which has been proven to be a suitable model for computing energies and molecular orbitals of organic dyes/TiO₂ systems.⁵⁻⁸ The dyes were anchored on the semiconductor using a bidentate bridging mode and the optimizations of the dye/TiO₂ systems were performed using the B3LYP/6-311G(d,p) level, in which the standard LANL2DZ basis set was used for the Ti atom. The absorption maximum (λ^a_{\max}), vertical excitation energy (E_{exc}), and oscillator strength (f) of dyes on TiO₂ were calculated on the optimized structures at the CAM-B3LYP/6-311G(d,p) level in which the standard LANL2DZ basis set was used for the Ti atom.

Concerning fluorescence emission, the lowest singlet state optimized geometries were computed at TD-CAM-B3LYP/6-31G* level of theory. The emission maxima (λ^e_{\max}), vertical emission energies (E_{emi}), oscillator strengths (f), and composition (%) in terms of molecular orbitals for the lowest singlet-singlet emissions in THF have been computed on the minimized structures at TD-CAM-B3LYP/6-311+G(2d,p) level of theory. Solvent effects have been included by using the Linear-Response implementation (LR-PCM).

2. Synthesis of the new dyes

2.1. Materials and methods

Unless otherwise stated, all reagents were purchased from commercial suppliers and used without purification. Dithieno[3,2-*b*:2',3'-*d*]pyrroles **1**,⁹ **5**, and **7**¹⁰ and bromide **2**¹¹ were prepared as previously reported. All air-sensitive reactions were performed using Schlenk techniques. Solvents used in cross-coupling reactions were previously degassed using the “freeze-pump-thaw” method. Toluene was dried on a resin exchange Solvent Purification System (*MBraun*). Petroleum ether, unless specified, is the 40-70°C boiling fraction. Reactions were monitored by TLC using silica gel 60 F254 aluminum sheet (Merck); the detection was made using a KMnO₄ basic solution or UV lamp. The organic phase derived from aqueous work-up was dried over Na₂SO₄. Flash column chromatography was performed using glass columns (10-50 mm wide) and Silica Gel 60 (230-400 mesh). ¹H-NMR spectra were recorded at 400 MHz and ¹³C-NMR spectra were recorded at 100.6 MHz, respectively, on *Bruker Avance* series instruments. Chemical shifts were referenced to the residual solvent peak (CDCl₃, δ 7.26 ppm for ¹H-NMR and δ 77.16 ppm for ¹³C-NMR; CD₂Cl₂, δ 5.32 ppm for ¹H-NMR and δ 53.84 ppm for ¹³C-NMR; THF-*d*₈ δ 1.72 and 3.58 ppm for ¹H-NMR, δ 67.21 and 25.31 ppm for ¹³C-NMR). Coupling constants (*J*) were reported in Hz. ESI-MS analyses were recorded with LCQ-Fleet Ion-Trap Mass Spectrometer (Thermo). HR-MS analyses were performed at CISM (Mass Spectrometry Center – University of Florence) using an LTQ Orbitrap FT- MS Spectrometer (Thermo). FT-IR spectra were recorded with a *Perkin-Elmer Spectrum BX* instrument in the range 4000-400 cm⁻¹ with a 2 cm⁻¹ resolution.

2.2. Synthetic procedures

6-(7-Bromobenzo[*c*][1,2,5]thiadiazol-4-yl)-4-hexyl-4*H*-dithieno[3,2-*b*:2',3'-*d*]pyrrole-2-carbaldehyde (4). Compound **1** (0.217 g, 0.745 mmol, 1.0 eq.), Pd(OAc)₂ (3.3 mg, 0.015 mmol, 2.0 mol%), CataCXium[®] A (11 mg, 0.03 mmol, 4.0 mol%), pivalic acid (23 mg, 0.223 mmol, 30 mol%), Cs₂CO₃ (0.364 g, 1.12 mmol, 1.5 eq.) and 4,7-dibromobenzo[*c*][1,2,5]thiadiazole (0.328 g, 1.12 mmol, 1.5 eq.) were dissolved in toluene (3.5 mL). The reaction mixture was stirred at 110 °C for 4 hours, cooled down to room temperature and filtered over Celite[®]. The filter cake was washed with dichloromethane (50 mL), the filtrate was evaporated under vacuum, then flash column chromatography (petroleum ether / dichloromethane gradient 1:1 to 1:3, then dichloromethane) afforded pure compound **4** (0.148 g, 0.293 mmol, 39% yield) as an orange solid. ¹H-NMR (300 MHz, CDCl₃): δ = 9.91 (s, 1H), 8.29 (s, 1H), 7.88 (d, *J* = 8.1 Hz, 1H), 7.75 (d, *J* = 7.3 Hz, 1H), 7.66 (s, 1H), 4.32 (t, *J* = 6.2 Hz, 2H), 1.87–2.03 (m, 2H), 1.24–1.46 (m, 6H), 0.81–0.95 (m, 3H) ppm; ¹³C-NMR (75 MHz, CDCl₃): δ = 183.1, 154.1, 151.7, 149.7, 145.1, 141.4, 141.1, 132.5, 127.7, 125.8, 119.3, 115.6, 114.7, 113.0, 112.7, 47.7, 31.5, 30.5, 26.8, 22.6, 14.2 ppm; IR (KBr): $\tilde{\nu}$ = 3066, 2925, 2853, 2803, 1649, 1533, 1491, 1389, 1355, 1219, 1185, 1140, 811 cm⁻¹; ESI-MS: *m/z* = 568.20 [M + CH₃CN + Na]⁺.

6-(7-(4-(diphenylamino)phenyl)benzo[*c*][1,2,5]thiadiazol-4-yl)-4-hexyl-4*H*-dithieno[3,2-*b*:2',3'-*d*]pyrrole-2-carbaldehyde (3). Compound **2** (1.20 g, 2.38 mmol, 1.0 eq.), (4-(diphenylamino)phenyl)boronic acid (0.758 g, 2.62 mmol, 1.1 eq.), Pd[(PPh₃)₄] (0.138 g, 0.119 mmol, 5.0 mol%) and a 2M aqueous solution of Na₂CO₃ (1.26 g, 6.0 mL, 12.0 mmol, 5.0 eq.) were mixed in toluene (50 mL). The resulting mixture was stirred at 100 °C for 16 hours, then, after cooling to room temperature, the solvent was removed under reduced pressure. The crude was dissolved in CH₂Cl₂ (200 mL) and washed with water (100 mL) and brine (100 mL), then the organic layer was dried with sodium sulfate. After filtration and removal of the solvent under vacuum, the crude was purified by flash column chromatography (Toluene, then dichloromethane). Pure aldehyde **3** (1.39 g, 2.08 mmol, 87% yield) was isolated as a purple solid. ¹H-NMR (400 MHz, CDCl₃): δ = 9.88 (s, 1H), 8.31 (s, 1H), 7.95 (d, *J* = 7.6 Hz, 1H), 7.88 (d, *J* = 8.2 Hz, 2H), 7.71 (d, *J* = 7.6 Hz, 1H), 7.64 (s, 1H), 7.27–7.35 (m, 4H), 7.16–7.24 (m, 6H), 7.05–7.12 (m, 2H), 4.32 (t, *J* = 7.3 Hz, 2H), 1.96 (q, *J* = 7.1 Hz, 2H), 1.25–1.45 (m, 6H), 0.84–0.92 (m, 3H) ppm; ¹³C-NMR (100 MHz, CDCl₃): δ = 183.0, 154.2, 152.8, 149.9, 148.4, 147.5, 144.9, 142.5, 140.9, 133.0, 130.5, 130.1, 129.6, 127.2, 126.2, 126.1, 125.2, 123.6, 123.4, 122.8, 119.2, 115.2, 111.9, 47.7, 31.5, 30.4, 26.8, 22.7, 14.2 ppm; IR (KBr): $\tilde{\nu}$ = 3032, 2928, 2855, 1642, 1588, 1489, 1340, 1277, 1177, 822, 698 cm⁻¹; ESI-MS: *m/z* = 688.18 [M]⁺.

4-(2',6'-bis(octyloxy)-[1,1'-biphenyl]-4-yl)-6-(7-(4-(diphenylamino)phenyl)benzo[*c*][1,2,5]thiadiazol-4-yl)-4*H*-dithieno[3,2-*b*:2',3'-*d*]pyrrole-2-carbaldehyde (6). Pd(OAc)₂ (2.2 mg, 0.010 mmol, 5.0 mol%), CataCXium® A (7.2 mg, 0.020 mmol, 10 mol%), pivalic acid (6.1 mg, 0.060 mmol, 30 mol%), Cs₂CO₃ (0.081 g, 0.25 mmol, 1.25 eq.), aldehyde **5** (0.123 g, 0.20 mmol, 1.0 eq.) and bromide **2** (0.092 g, 0.20 mmol, 1.0 eq.) were mixed with toluene (2.0 mL). The resulting mixture was heated up to 110 °C and stirred for 16 hours, then cooled down to room temperature and filtered over Celite®. The filter cake was washed with dichloromethane (50 mL), then the solvent was evaporated and the crude was purified by flash column chromatography (petroleum ether / dichloromethane gradient 2:1 to 1:3), which afforded pure aldehyde **6** (146 mg, 0.147 mmol, 74% yield) as a dark purple solid. ¹H-NMR (400 MHz, CDCl₃): δ = 9.89 (s, 1H), 8.44 (s, 1H), 7.97 (d, *J* = 7.3 Hz, 1H), 7.88 (d, *J* = 8.4 Hz, 2H), 7.85 (s, 1H), 7.72 (d, *J* = 7.3 Hz, 1H), 7.66 (s, 4H), 7.27–7.34 (m, 5H), 7.16–7.22 (m, 6H), 7.08 (t, *J* = 7.2 Hz, 2H), 6.69 (d, *J* = 8.4 Hz, 2H), 3.98 (t, *J* = 6.4 Hz, 4H), 1.70 (q, *J* = 6.8 Hz, 4H), 1.30–1.40 (m, 4H), 1.13–1.29 (m, 16H), 0.71–0.79 (m, 6H) ppm; ¹³C-NMR (100 MHz, CDCl₃): δ = 183.1, 157.3, 154.1, 152.7, 148.7, 148.4, 147.5, 144.0, 142.7, 141.3, 136.9, 133.4, 133.2, 133.1, 130.5, 130.1, 129.5, 129.2, 127.2, 126.1, 126.0, 125.2, 125.0, 123.6, 122.8, 121.9, 121.1, 118.8, 117.1, 112.9, 105.4, 68.8, 31.9, 29.4, 29.3, 29.2, 26.1, 22.7, 14.2 ppm; IR (KBr): $\tilde{\nu}$ = 3033, 2929, 2848, 1649, 1594, 1487, 1399, 1273, 1093, 823, 689 cm⁻¹; ESI-MS: *m/z* = 992.20 [M]⁺.

4-(4-(2',6'-bis(octyloxy)-[1,1'-biphenyl]-4-yl)-6-(7-(4-(diphenylamino)phenyl)benzo[*c*][1,2,5]thiadiazol-4-yl)-4*H*-dithieno[3,2-*b*:2',3'-*d*]pyrrol-2-yl)benzaldehyde (8). Compound **7** (0.117 g, 0.20 mmol, 1.0 eq.), bromide **2** (0.092 g, 0.20 mmol, 1.0 eq.), Pd(OAc)₂ (2.2 mg, 0.010 mmol, 5.0 mol%), CataCXium® A (7.2 mg,

0.020 mmol, 10 mol%), pivalic acid (6.1 mg, 0.060 mmol, 30 mol%) and Cs₂CO₃ (0.078 g, 0.24 mmol, 1.2 eq.), were dissolved in toluene (2.0 mL). The reaction mixture was stirred at 110 °C for 8 hours, then 4-bromobenzaldehyde (44 mg, 0.24 mmol, 1.2 eq.) and another portion of Cs₂CO₃ (0.078 g, 0.24 mmol, 1.2 eq.) were added. The heating was prolonged for additional 16 hours, then the mixture was cooled down to room temperature and filtered over Celite®. The filter cake was washed with dichloromethane (50 mL), the filtrate was evaporated under vacuum, then flash column chromatography (petroleum ether / dichloromethane gradient 4:1 to 1:3) afforded pure compound **8** (55 mg, 0.052 mmol, 26% yield) as a dark purple solid. ¹H-NMR (400 MHz, CD₂Cl₂): δ = 9.95 (s, 1H); 8.45 (s, 1H); 7.93 (d, *J* = 7.3 Hz, 1H); 7.82–7.90 (m, 4H); 7.75–7.82 (m, 2H); 7.61–7.75 (m, 6H); 7.23–7.36 (m, 5H); 7.12–7.21 (m, 6H); 7.04–7.12 (m, 2H); 6.70 (d, *J* = 8.4 Hz, 2H); 3.98 (t, *J* = 6.4 Hz, 4H); 1.63–1.77 (m, 4H); 1.07–1.43 (m, 20H); 0.73 (t, *J* = 6.6 Hz, 6H) ppm; ¹³C-NMR (100 MHz, CD₂Cl₂): δ = 191.4, 157.6, 154.4, 153.0, 148.4, 147.8, 145.7, 145.4, 141.33, 141.31, 139.4, 137.7, 135.3, 133.4, 133.3, 132.2, 131.1, 130.7, 130.3, 129.8, 129.4, 127.4, 126.7, 125.5, 125.34, 125.27, 123.8, 123.0, 122.0, 119.0, 118.4, 117.9, 113.3, 110.6, 105.6, 69.0, 32.2, 29.7, 29.6, 29.5, 26.4, 23.0, 14.2 ppm; IR (KBr): $\tilde{\nu}$ = 3018, 2915, 2841, 1690, 1594, 1487, 1399, 1281, 1100, 816, 694 cm⁻¹; ESI-MS: *m/z* = 1068.19 [M]⁺.

General procedure for the preparation of compounds **BTD-DTP1–3**

The appropriate aldehyde (**3**, **6** or **8**, 1.0 eq.) was dissolved in toluene and glacial acetic acid (2:1 v/v), then cyanoacetic acid (5.0 eq.) and ammonium acetate (1.5 eq.) were added. The resulting mixture was stirred at 110 °C for 4 hours, then cooled down to room temperature. After dilution with additional toluene, the organic phase was washed twice with HCl_(aq.) 0.3 M and the solvent evaporated. The resulting solid was purified by washing with several portions of *n*-pentane, ethyl acetate, and methanol, and dried under vacuum.

(E)-2-cyano-3-(6-(7-(4-(diphenylamino)phenyl)benzo[c][1,2,5]thiadiazol-4-yl)-4-hexyl-4H-dithieno[3,2-b:2',3'-d]pyrrol-2-yl)acrylic acid (BTD-DTP1). According to the general procedure, aldehyde **3** (1.50 g, 2.24 mmol) was dissolved in toluene (20 mL) and acetic acid (10 mL) and reacted with cyanoacetic acid (0.954 g, 11.2 mmol) and NH₄OAc (0.259 g, 3.36 mmol) for 4 hours. Work-up and purification afforded dye **BTD-DTP1** (1.41 g, 1.92 mmol, 85% yield) as an amorphous black solid. ¹H-NMR (400 MHz, THF-*d*₈): δ = 8.47 (s, 1H), 8.34 (s, 1H), 8.08 (d, *J* = 7.3 Hz, 1H), 8.00 (d, *J* = 8.8 Hz, 2H), 7.92 (s, 1H), 7.83 (d, *J* = 7.3 Hz, 1H), 7.24–7.34 (m, 4H), 7.12–7.20 (m, 6H), 7.00–7.10 (m, 2H), 4.41 (t, *J* = 6.6 Hz, 2H), 1.94–2.04 (m, 2H), 1.26–1.44 (m, 6H), 0.83–0.94 (m, 3H) ppm; ¹³C-NMR (100 MHz, THF-*d*₈): δ = 164.4, 154.7, 153.4, 150.8, 149.0, 148.3, 147.7, 146.1, 143.5, 135.0, 133.2, 131.4, 130.7, 130.0, 127.6, 126.8, 126.5, 125.5, 124.8, 124.0, 123.3, 120.8, 117.1, 116.2, 112.4, 96.1, 47.8, 32.2, 30.9, 27.4, 23.3, 14.2 ppm; IR (KBr): $\tilde{\nu}$ = 3439, 3033, 2915, 2848, 2206, 1671, 1576, 1491, 1258, 1177, 816, 694 cm⁻¹; HRMS (ESI) for C₄₂H₃₃N₅O₂S₃ [M]⁺: calcd. 735.17909, found: 735.17888 *m/z*.

(E)-3-(4-(2',6'-bis(octyloxy)-[1,1'-biphenyl]-4-yl)-6-(7-(4-(diphenylamino)phenyl)benzo[c][1,2,5]thiadiazol-4-yl)-4H-dithieno[3,2-b:2',3'-d]pyrrol-2-yl)-2-cyanoacrylic acid (BTD-DTP2). According to the general procedure, aldehyde **6** (120 mg, 0.121 mmol) was dissolved in toluene (3.0 mL) and acetic acid (1.5 mL) and

reacted with cyanoacetic acid (51 mg, 0.604 mmol) and NH₄OAc (14 mg, 0.181 mmol) for 4 hours. Work-up and purification afforded dye **BTD-DTP2** (126 mg, 0.119 mmol, 98% yield) as an amorphous black solid. ¹H-NMR (400 MHz, THF-*d*₈): δ = 8.53 (s, 1H), 8.38 (s, 1H), 8.08 (d, *J* = 7.6 Hz, 1H), 8.00 (s, 1H), 7.95 (d, *J* = 8.6 Hz, 2H), 7.79 (d, *J* = 7.6 Hz, 1H), 7.74 (d, *J* = 8.4 Hz, 2H), 7.65 (d, *J* = 8.4 Hz, 2H), 7.20–7.32 (m, 5H), 7.08–7.19 (m, 6H), 7.04 (t, *J* = 8.4 Hz, 2H), 6.71 (d, *J* = 8.4 Hz, 2H), 3.95 (t, *J* = 6.4 Hz, 4H), 1.67 (q, *J* = 6.8 Hz, 4H), 1.32–1.42 (m, 4H), 1.10–1.31 (m, 16H), 0.69–0.80 (m, 6H) ppm; ¹³C-NMR (100 MHz, THF-*d*₈): δ = 164.4, 158.0, 154.6, 153.3, 149.2, 148.9, 148.3, 147.6, 144.8, 143.7, 137.5, 135.6, 134.2, 133.8, 133.3, 131.3, 130.7, 130.0, 129.5, 127.5, 126.6, 126.5, 126.3, 125.5, 124.0, 123.2, 122.4, 122.0, 119.5, 118.1, 117.1, 113.3, 105.9, 97.0, 69.1, 32.6, 30.1, 30.0, 29.9, 26.8, 23.3, 14.2 ppm; IR (KBr): $\tilde{\nu}$ = 3453, 3033, 2922, 2856, 2206, 1664, 1572, 1487, 1380, 1251, 1159, 1096, 816, 698 cm⁻¹; HRMS (ESI) for C₆₄H₆₁N₅O₄S₃ [M]⁺: calcd. 1059.38802, found: 1059.38610 *m/z*.

(E)-3-(4-(4-(2',6'-bis(octyloxy)-[1,1'-biphenyl]-4-yl)-6-(7-(4-(diphenylamino)phenyl)benzo[*c*][1,2,5]thiadiazol-4-yl)-4H-dithieno[3,2-*b*:2',3'-*d*]pyrrol-2-yl)phenyl)-2-cyanoacrylic acid (BTD-DTP3). According to the general procedure, aldehyde **8** (50 mg, 0.047 mmol) was dissolved in toluene (2.0 mL) and acetic acid (1.0 mL) and reacted with cyanoacetic acid (20 mg, 0.234 mmol) and NH₄OAc (5.4 mg, 0.070 mmol) for 4 hours. Work-up and purification afforded dye **BTD-DTP3** (41 mg, 0.036 mmol, 77% yield) as an amorphous black solid. ¹H-NMR (400 MHz, THF-*d*₈): δ = 8.55 (s, 1H); 8.22 (s, 1H); 8.09 (d, *J* = 8.4 Hz, 2H); 8.04 (d, *J* = 7.6 Hz, 1H); 7.97 (d, *J* = 8.4 Hz, 2H); 7.83–7.91 (m, 3H); 7.74–7.82 (m, 3H); 7.65 (d, *J* = 8.4 Hz, 2H); 7.22–7.32 (m, 5H); 7.09–7.19 (m, 6H); 7.00–7.08 (m, 2H); 6.71 (d, *J* = 8.4 Hz, 2H); 3.92 (t, *J* = 6.2 Hz, 4H); 1.63–1.72 (m, 4H); 1.33–1.44 (m, 4H); 1.12–1.32 (m, 16H); 0.67–0.78 (m, 6H) ppm; ¹³C-NMR (100 MHz, THF-*d*₈): δ = 163.8, 158.0, 154.7, 153.4, 153.3, 148.8, 148.4, 146.2, 146.0, 141.9, 140.5, 139.8, 138.0, 133.9, 133.7, 132.5, 132.4, 131.7, 131.3, 130.7, 130.0, 129.5, 127.7, 127.2, 125.8, 125.6, 125.5, 123.9, 123.4, 122.1, 119.7, 118.8, 118.5, 116.4, 113.7, 111.2, 105.9, 103.2, 69.1, 32.6, 30.1, 30.0, 29.9, 26.8, 23.3, 14.2 ppm; IR (KBr): $\tilde{\nu}$ = 3431, 3018, 2922, 2848, 2214, 1690, 1579, 1491, 1395, 1273, 1181, 1096, 816, 698 cm⁻¹; HRMS (ESI) for C₇₀H₆₅N₅O₄S₃ [M]⁺: calcd. 1135.41932, found: 1135.42119 *m/z*.

2.3. Additional details on the double direct arylation of compound **7**

As described in the main text, compound **7** was subjected to a sequential, Pd-catalyzed double direct arylation procedure with bromide **2** and 4-bromobenzaldehyde to provide advanced intermediate **8** in 26% yield. The moderate yield of aldehyde **8** is mainly due to the not-negligible formation of some co-products (Figure S1), which were nevertheless easily separated by chromatographic purification and identified by ¹H-NMR spectroscopy. In detail, mono-arylated products **9** and **10** were isolated with a yield of 16% and 9% respectively, while yields of symmetrical products **11** and **12** were 11% and 17%, respectively. Reversing the order of addition of the bromides (4-bromobenzaldehyde in the first step and bromide **2** in the second,

keeping the same catalytic conditions) did not change the yield of product **8**, which was again around 26%, but affected those of the co-products, which were 17%, 6%, 23% and 11% for **9**, **10**, **11** and **12**, respectively.

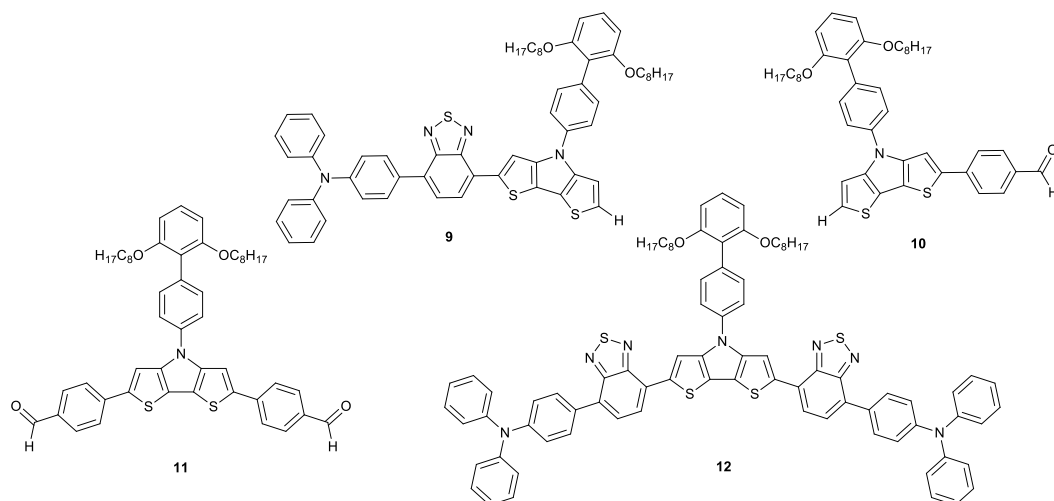


Figure S1. Co-products obtained in the transformation of DTP **7** to advanced intermediate **8**.

3. Spectroscopic and Electrochemical Measurements

UV-Vis spectra in different solvents were recorded on diluted solutions of the analyte (approximately 10^{-5} M) with a Shimadzu UV-2600 spectrometer. UV-vis absorption or transmittance spectra of the compounds adsorbed on TiO_2 were recorded with the same instrument in transmission mode after the sensitization of thin, transparent semiconductor films (thickness approximately 5 μm). Calculation of the weighted transparency (WT%) parameter in the 300-700 nm range was carried out according to the following equation:

$$WT(\%) = \frac{\int T(\lambda)I(\lambda)a(\lambda)d\lambda}{\int I(\lambda)a(\lambda)d\lambda} \times 100$$

where $T(\lambda)$ is the transmission of the semitransparent dye-sensitized semiconductor film, $I(\lambda)$ is the AM 1.5 solar spectral irradiance, and $a(\lambda)$ represents the action spectrum obtained from the combination of the normalized absorption spectra of chlorophyll a, chlorophyll b and beta-carotene, showed in Figure S5. Ultraviolet–Visible absorption diffuse reflectance spectra (DRS) of the dye-sensitized working electrodes were recorded using a Jasco V-770 spectrophotometer equipped with a 60 mm integrating sphere, embedding a PbS detector (ISN-923), using an interval wavelength of 1 nm, from 300 nm to 800 nm.

4. Dye-Sensitized Solar Cells Fabrication and Characterization

4.1. Materials

Fluorine-doped tin oxide glass (TEC 8, 3.2 mm thickness, Pilkington), titania paste for blocking layer (BL-1 Blocking Layer, Dyesol), titanium dioxide nano-powder (P25, Degussa), titanium (IV) chloride (purity $\geq 99\%$, Sigma Aldrich), industry-standard ruthenium-based dye (N719, Dyesol), tetrahydrofuran (analytical reagent

grade, Fisher Chemical), chlorobenzene (purex analytical grade, Merck), ethanol absolute (analytical reagent grade, Fisher Chemical), iodide-based high performance liquid state electrolyte (EL-HPE, Dyesol), platinum paste (PT1, Dyesol), low-temperature thermoplastic sealant (50 μm thickness, Dyesol), and silver paste (Electrodag 1415, Agar Scientific) were used.

4.2. Fabrication of the dye-sensitized solar cells

The working electrodes of the DSSCs consisted of a fluorine-doped tin oxide (FTO) glass of 3.2 mm thickness as the substrate, an ultra-thin TiO_2 compact layer as the blocking layer, and a TiO_2 thin mesoporous film sensitized by the different dyes as the main active layer. The blocking layer was fabricated by spin-coating the commercially available BL-1 Blocking layer paste on the FTO glass at 1500 rpm and firing of the system at 500 $^\circ\text{C}$ for 60 min. The main active layer was fabricated on the top of the blocking layer by spin-coating a homemade TiO_2 paste that was prepared by a simple chemical technique, as reported elsewhere.¹² Different mesoporous film thicknesses (15, 9, or 6 μm) were obtained by spin-coating the homemade TiO_2 paste, either by configuring the revolutions per minute of the coater or by using more layers. Subsequently, the nanostructured working electrodes were sintered at 525 $^\circ\text{C}$ for 90 min, followed by their gradual cooling to room temperature, leading to uniform semi-transparent mesoporous films, without cracking and peeling-off from the substrate. The TiCl_4 treatment was carried out by immersing the TiO_2 electrodes into a 40 mM TiCl_4 aqueous solution at 70 $^\circ\text{C}$ for 30 min, followed again by their sintering at 500 $^\circ\text{C}$ for 30 min and their gradual cooling to room temperature. The sensitization of the working electrodes was carried out by their immersion into a 0.1 mM **BTD-DTP1**, **BTD-DTP2**, and **BTD-DTP3** dyes tetrahydrofuran (THF) or chlorobenzene (CB) solution for 12 h, at room temperature. Working electrodes that employed the conventional **N719** dye as a sensitizer were also fabricated for comparison purposes. In this case, the sensitization of the working electrodes was carried out by their immersion in a 0.3 mM **N719** dye ethanolic (EtOH) solution for 24 h, at room temperature. The counter electrodes were fabricated by doctor-blading the PT1 paste on FTO glasses of 3.2 mm thickness and firing of the system at 500 $^\circ\text{C}$ for 30 min. Finally, the dye-sensitized working electrodes were sandwiched with the counter electrodes, separated by a low-temperature thermoplastic spacer/sealant of 50 μm thickness. The sealing was carried out at 120 $^\circ\text{C}$ for 15 min under a constant pressure given by two clips. The intervening space was filled with a drop of the liquid state EL-HPE electrolyte, through one hole that was already drilled to the counter electrodes. A special syringe facilitated the procedure through a vacuum and filling process. The fabrication procedure of the solar cells was completed by covering and sealing the hole that was drilled to the counter electrodes using an extra piece of glass under the same sealing conditions, while the contacts of the solar cells were fabricated using a silver paste to collect the current efficiently. In all cases, the active area of the solar cells was 0.25 cm^2 , corresponding to the aperture area of a proper shading mask that covered the rest of the electrode, preventing the light incidence from the

edges.¹³ Figure S7 shows the different colored working electrodes that were sensitized by the different dyes, as well as a cross-section of the solar cells.

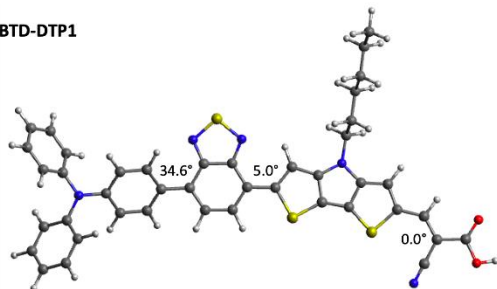
4.3. Characterization of the dye-sensitized solar cells

The solar cells were characterized under standard test conditions (1000 W/m², AM 1.5 G, 25 °C) using a Solar Light (16S-300) solar simulator calibrated by a reference cell consisting of monocrystalline silicon (Newport 919P-003-10); the photo-current density–voltage (J–V) curves of solar cells were recorded using Keithley 2601 source meter. Incident photon-to-electron conversion efficiency (IPCE) of the solar cells was determined by a ThetaMetrisis PM-QE equipped with a Xenon (Xe) light source, using a filter monochromator (Oriel Cornerstone™ 260 1/4 m, Newport), which was controlled by the PM-Monitor® software; the IPCE measurements were carried out using an interval wavelength of 5 nm and a delay time of 0.2 s, from 300 nm to 800 nm. Electrochemical impedance spectroscopy (EIS) measurements were carried out on the solar cells using a Metrohm Autolab 3.v potentiostat galvanostat (Model PGSTAT 128 N); the measurements were recorded in the dark at –VOC forward bias using a perturbation of ±10 mV, over the frequency range from 100 kHz to 0.1 Hz, at room temperature.

5. Additional Figures

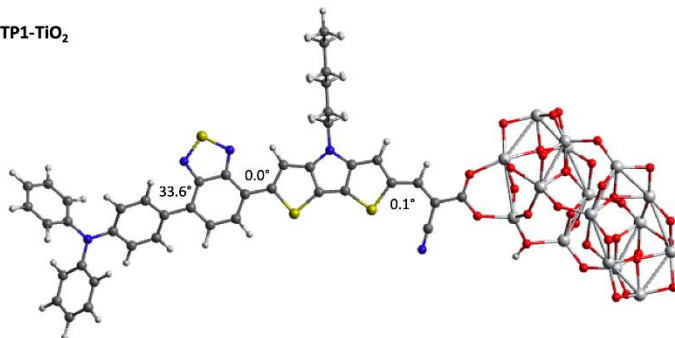
a)

BTD-DTP1

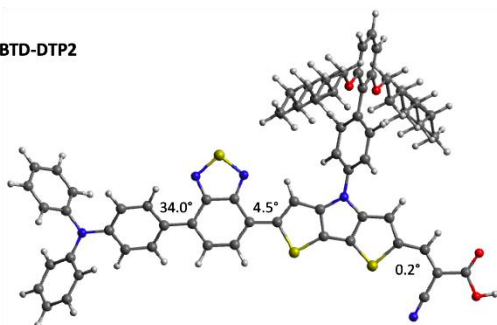


b)

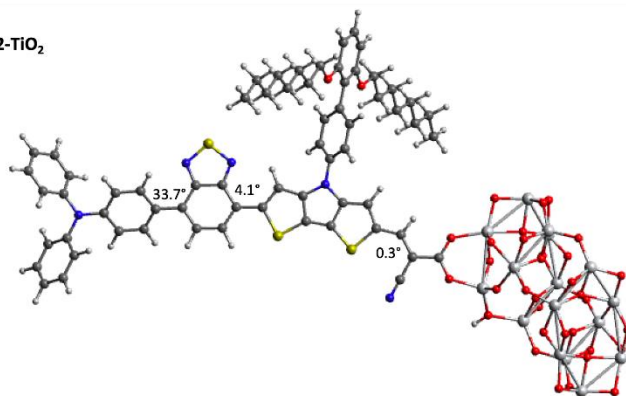
BTD-DTP1-TiO₂



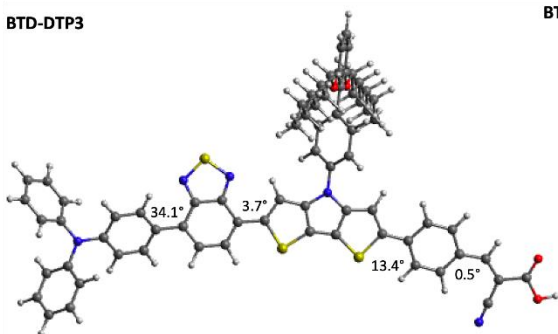
BTD-DTP2



BTD-DTP2-TiO₂



BTD-DTP3



BTD-DTP3-TiO₂

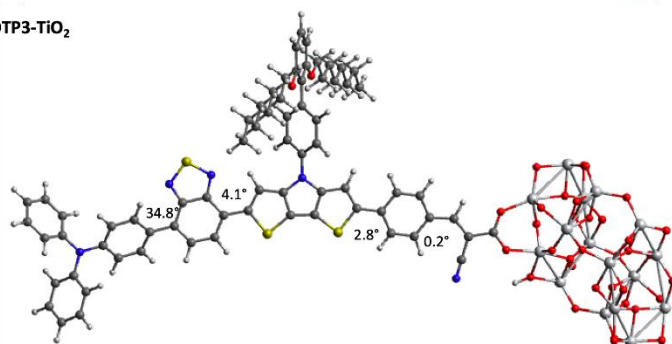


Figure S2. Ground state optimized geometries for dyes **BTD-DTP1-3** (a) in vacuum and (b) adsorbed on a $Ti_{16}O_{32}$ cluster (as a model of bulk TiO_2).

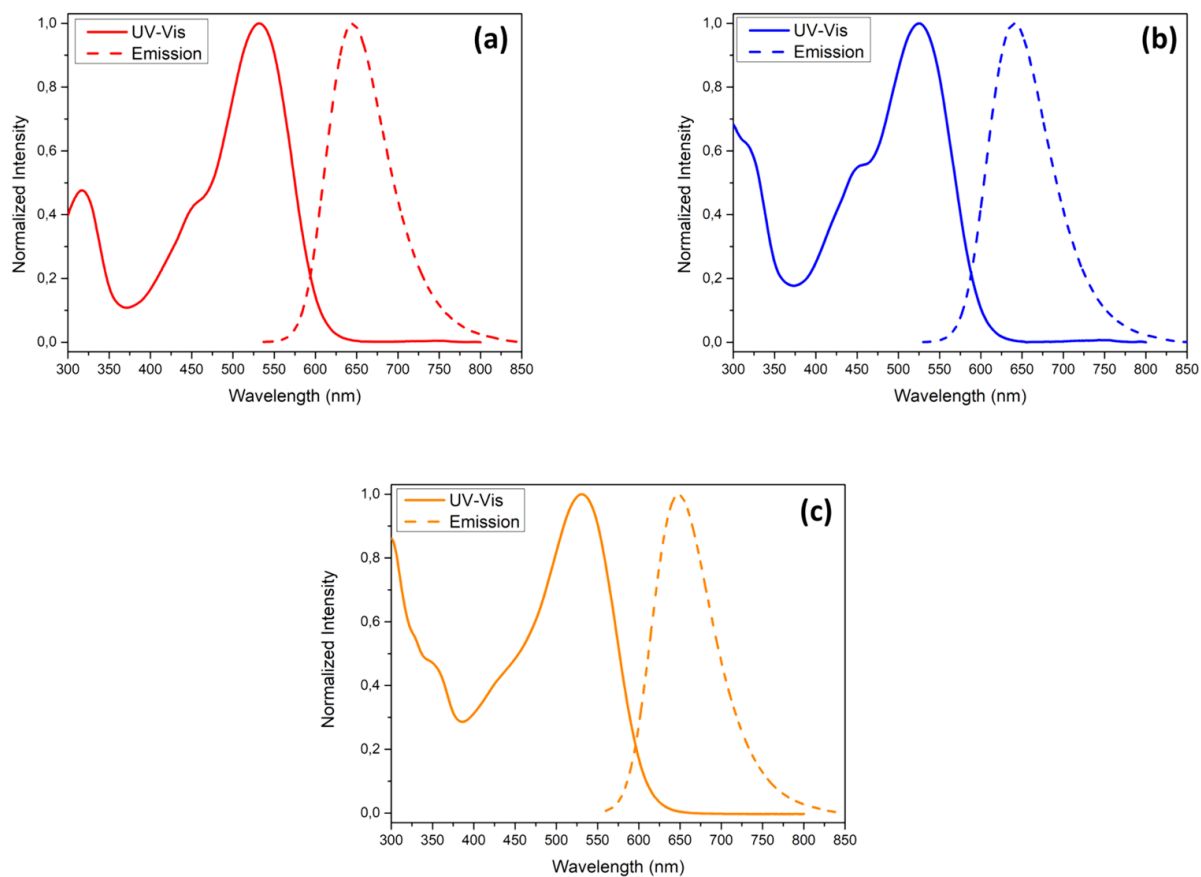


Figure S3. Normalized UV-Vis and fluorescence emission spectra of the new dyes in THF solution: (a) **BTD-DTP1**; (b) **BTD-DTP2**; (c) **BTD-DTP3**. Emission spectra were obtained by exciting the samples at the maximum absorption wavelength.

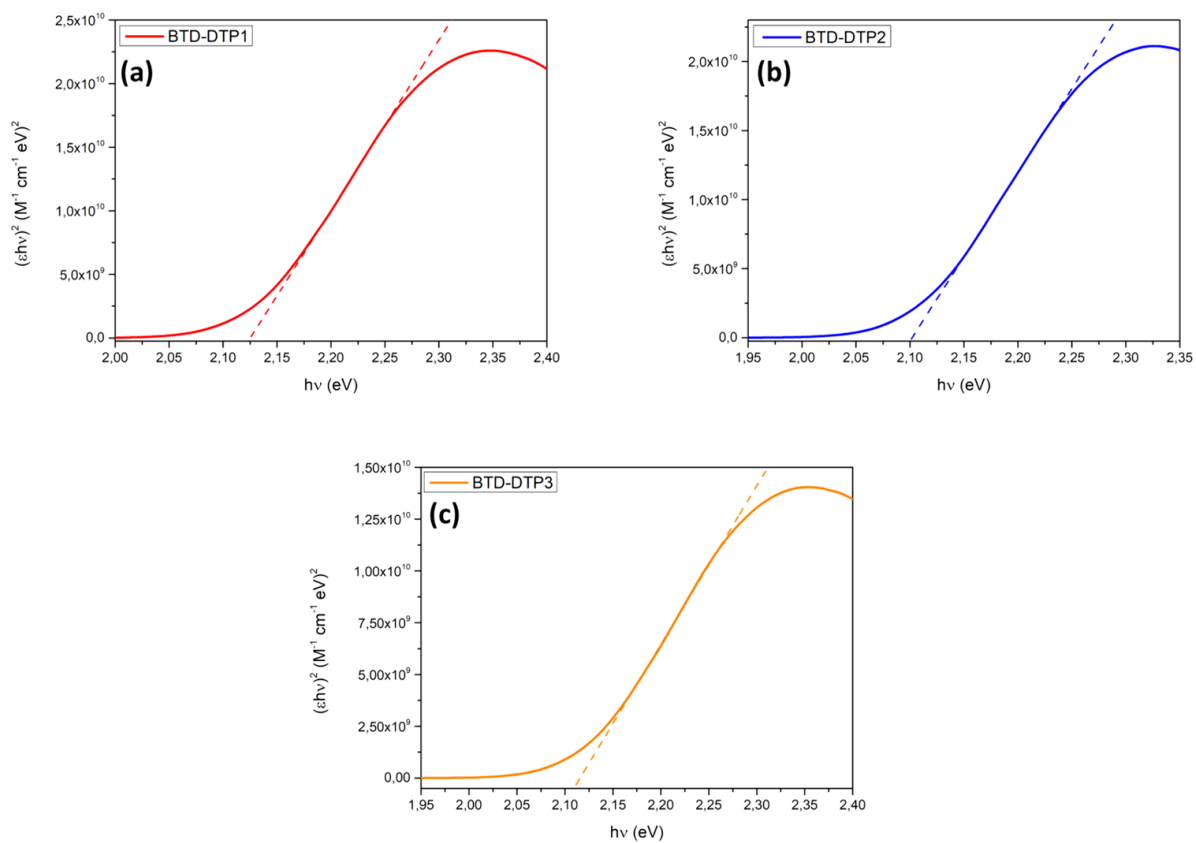


Figure S4. Tauc plots of the new dyes in THF solution: (a) **BTD-DTP1**; (b) **BTD-DTP2**; (c) **BTD-DTP3**.

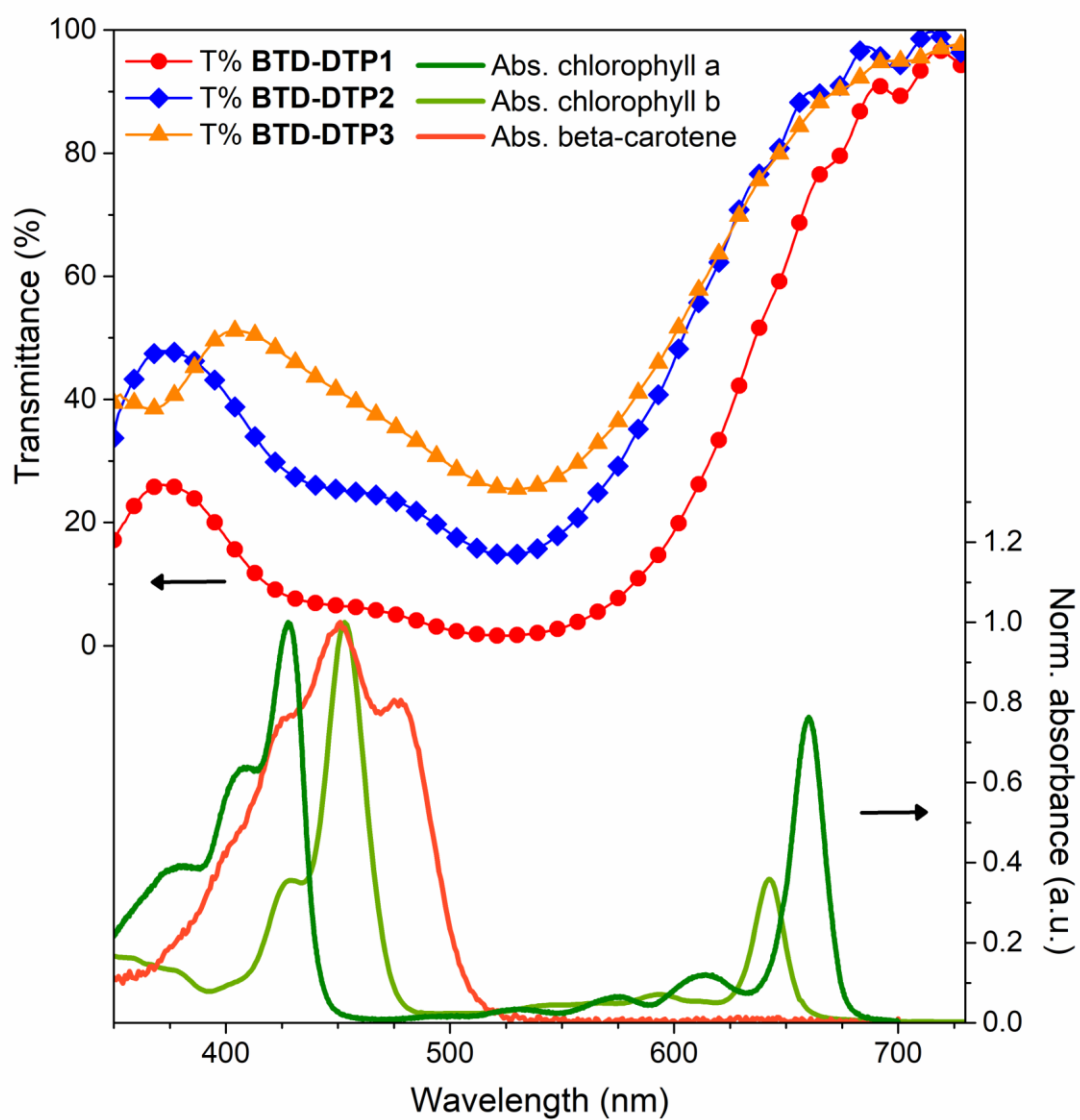


Figure S5. Comparison between the transmission spectra of dyes **BTD-DTP1-3** adsorbed on thin transparent TiO_2 films and the UV-Vis absorption spectra of the most common plant photoreceptors (chlorophyll a, chlorophyll b, beta carotene).

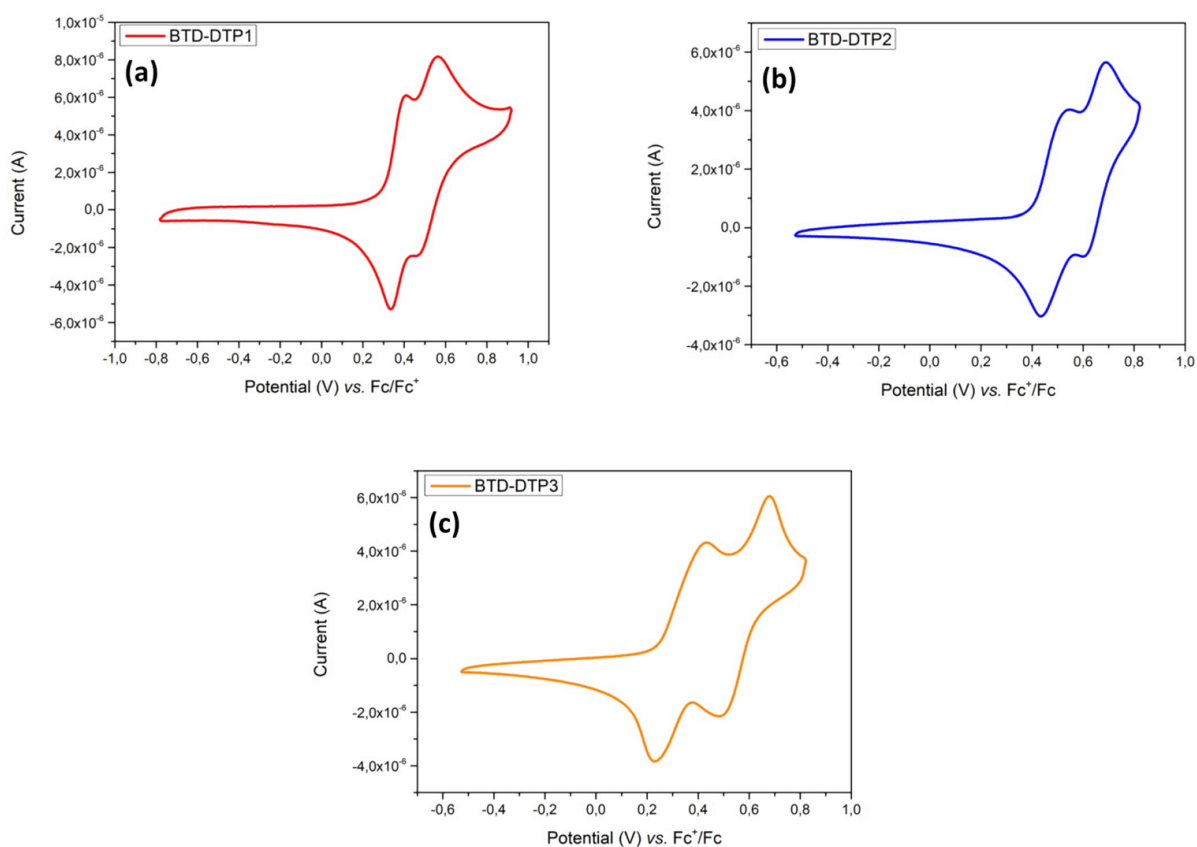


Figure S6. Cyclic voltammetry plots of the new dyes in CHCl_3 solution: (a) **BTD-DTP1**; (b) **BTD-DTP2**; (c) **BTD-DTP3**.

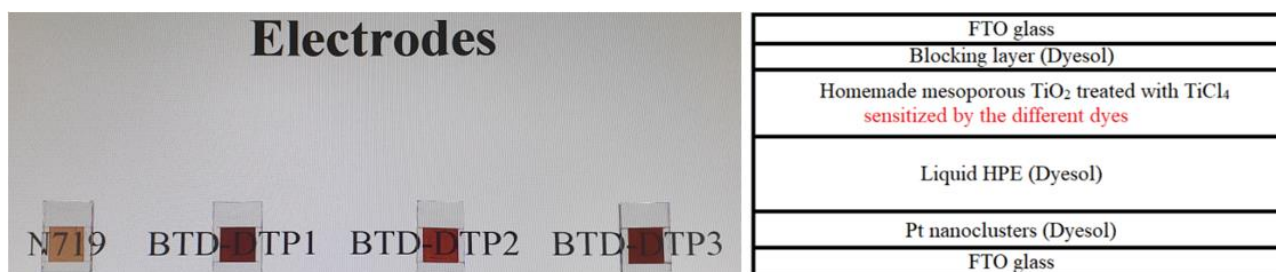
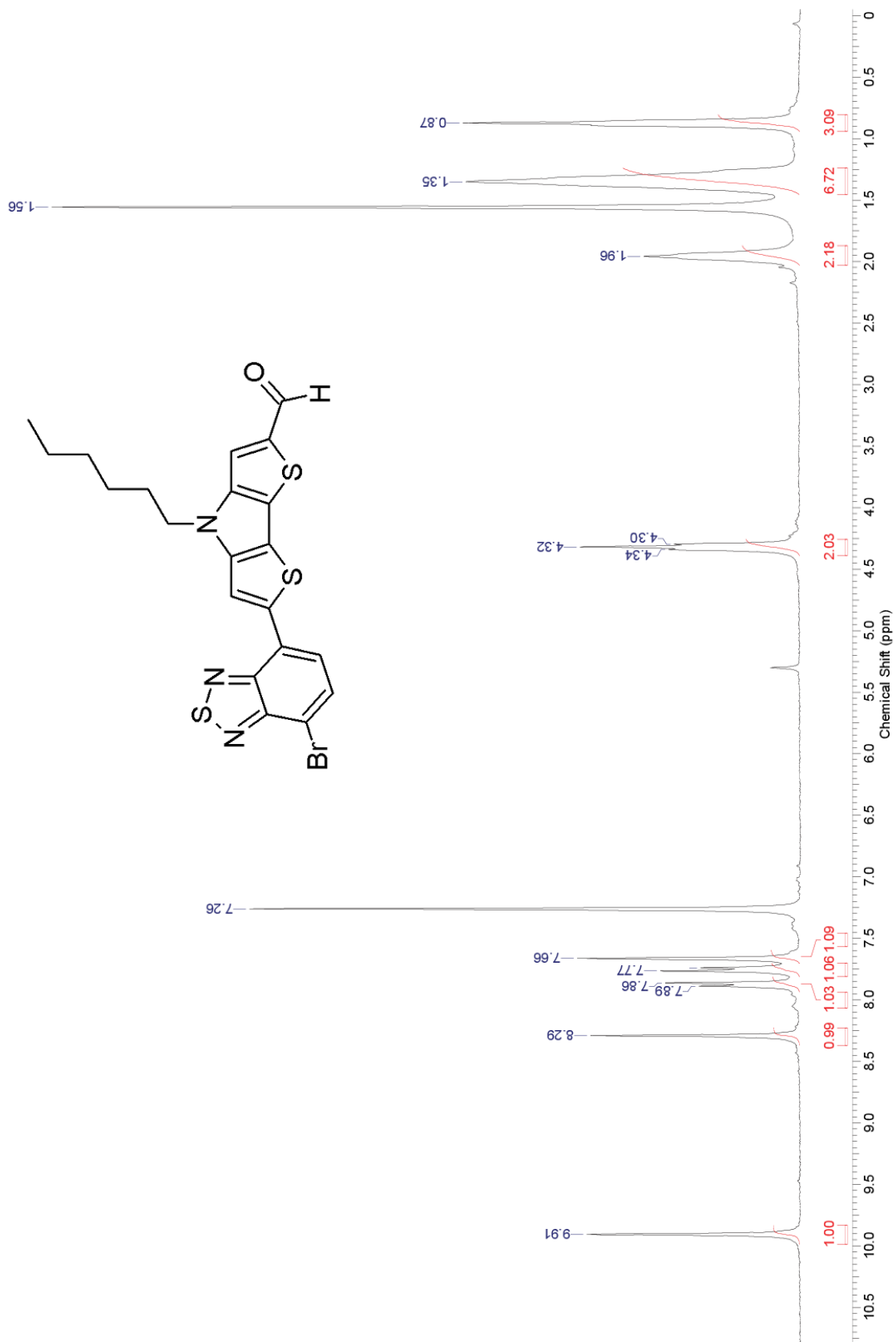
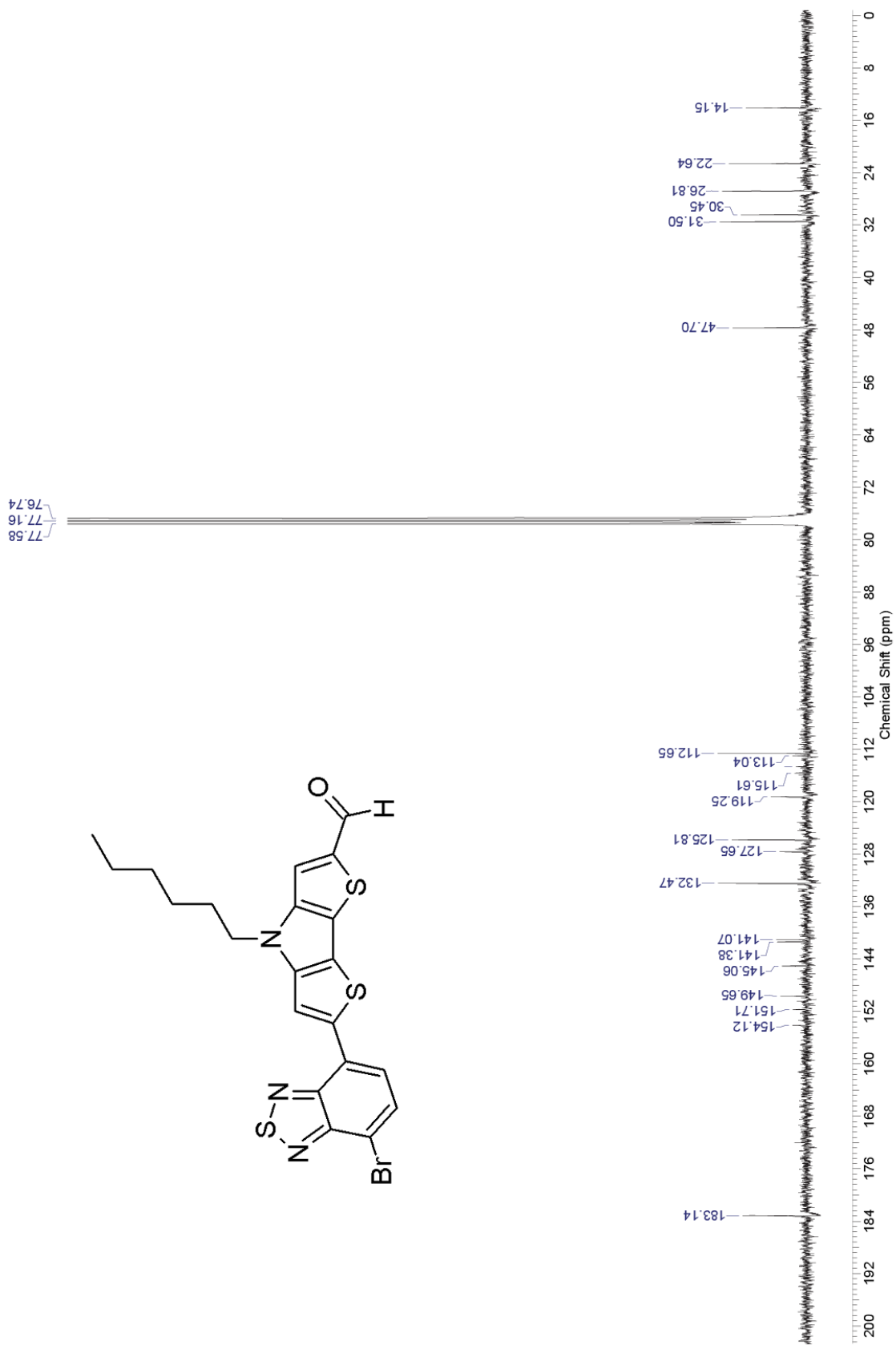
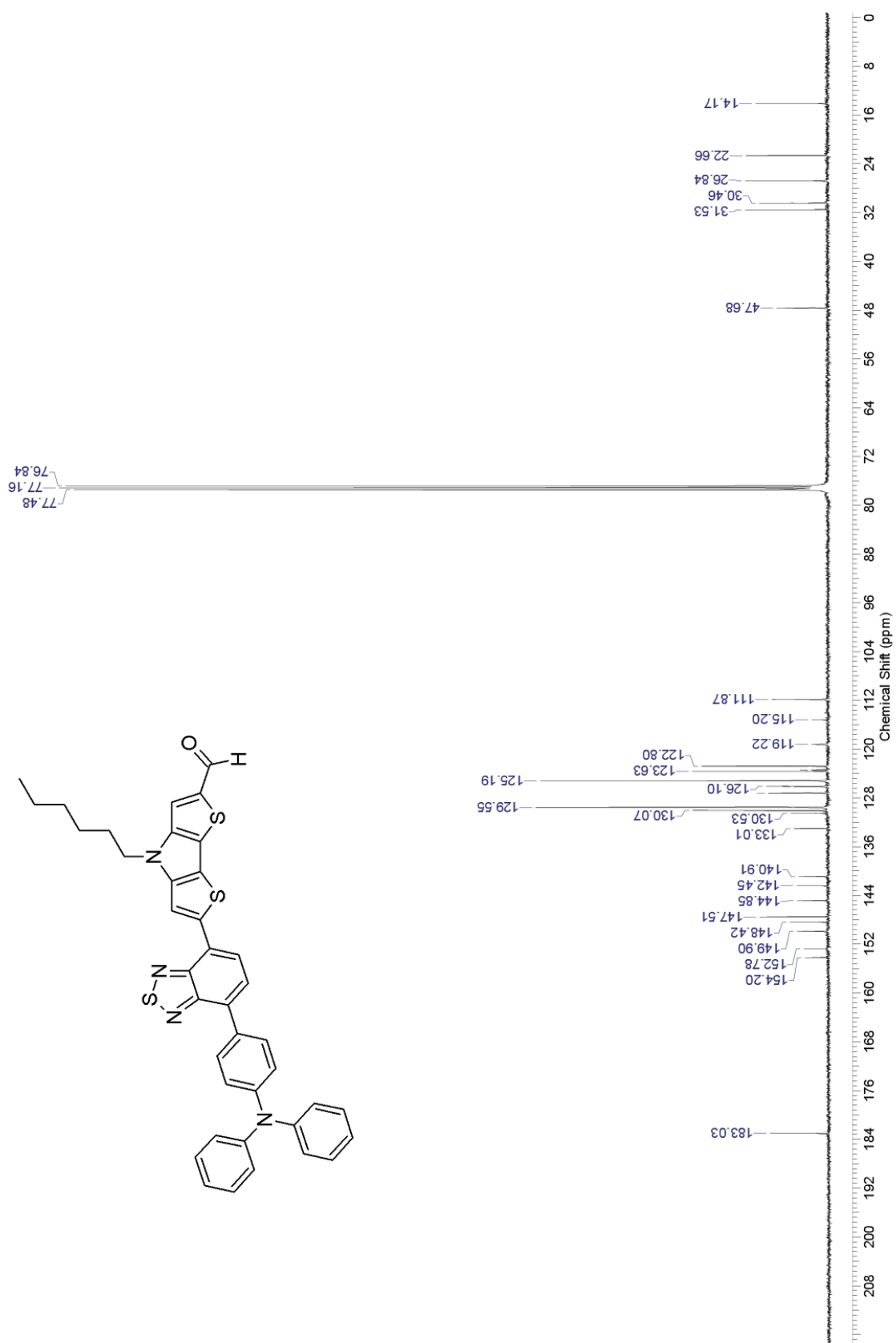


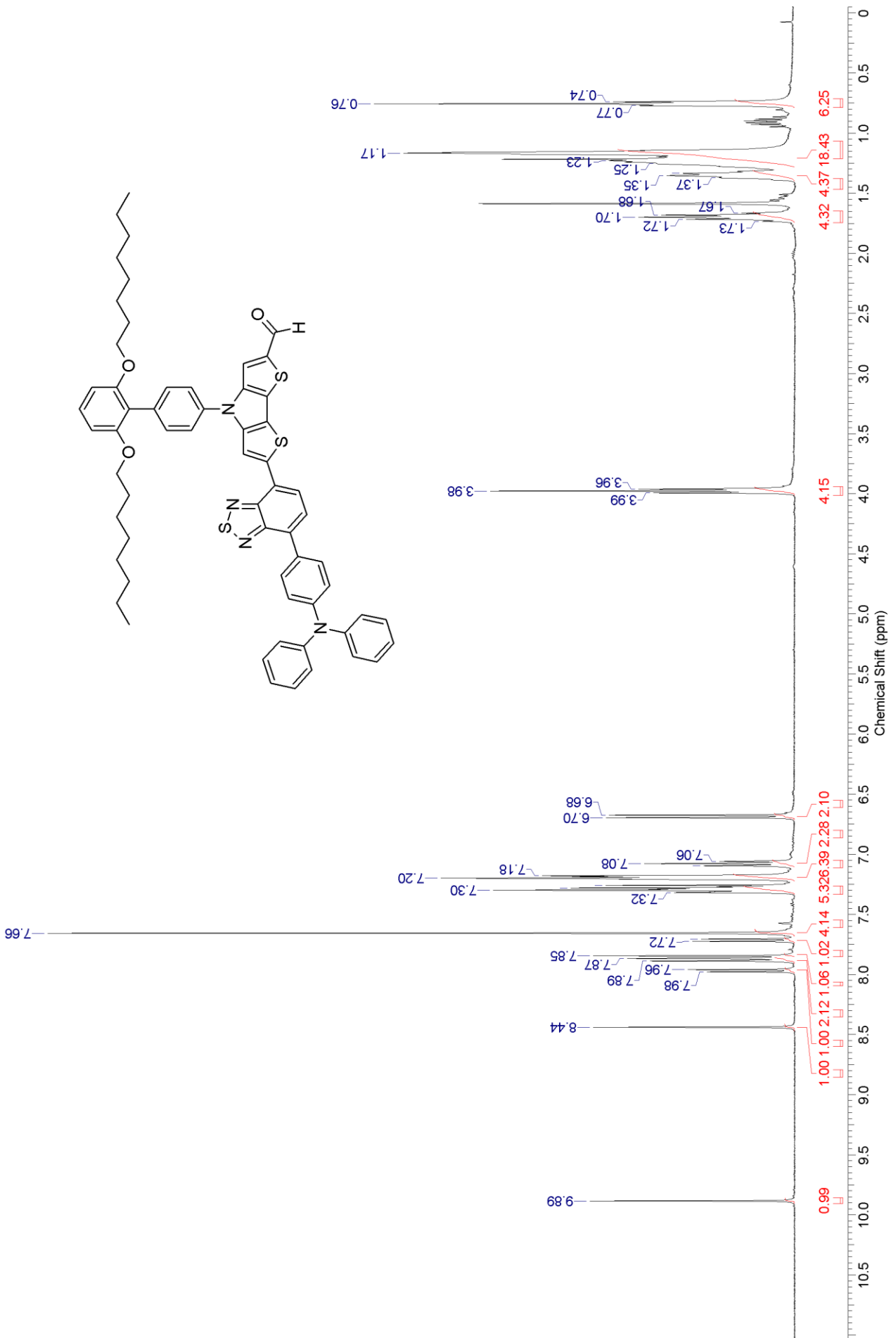
Figure S7. Dye-sensitized working electrodes ($6 \mu\text{m}$ thickness) and cross-section of the solar cells.

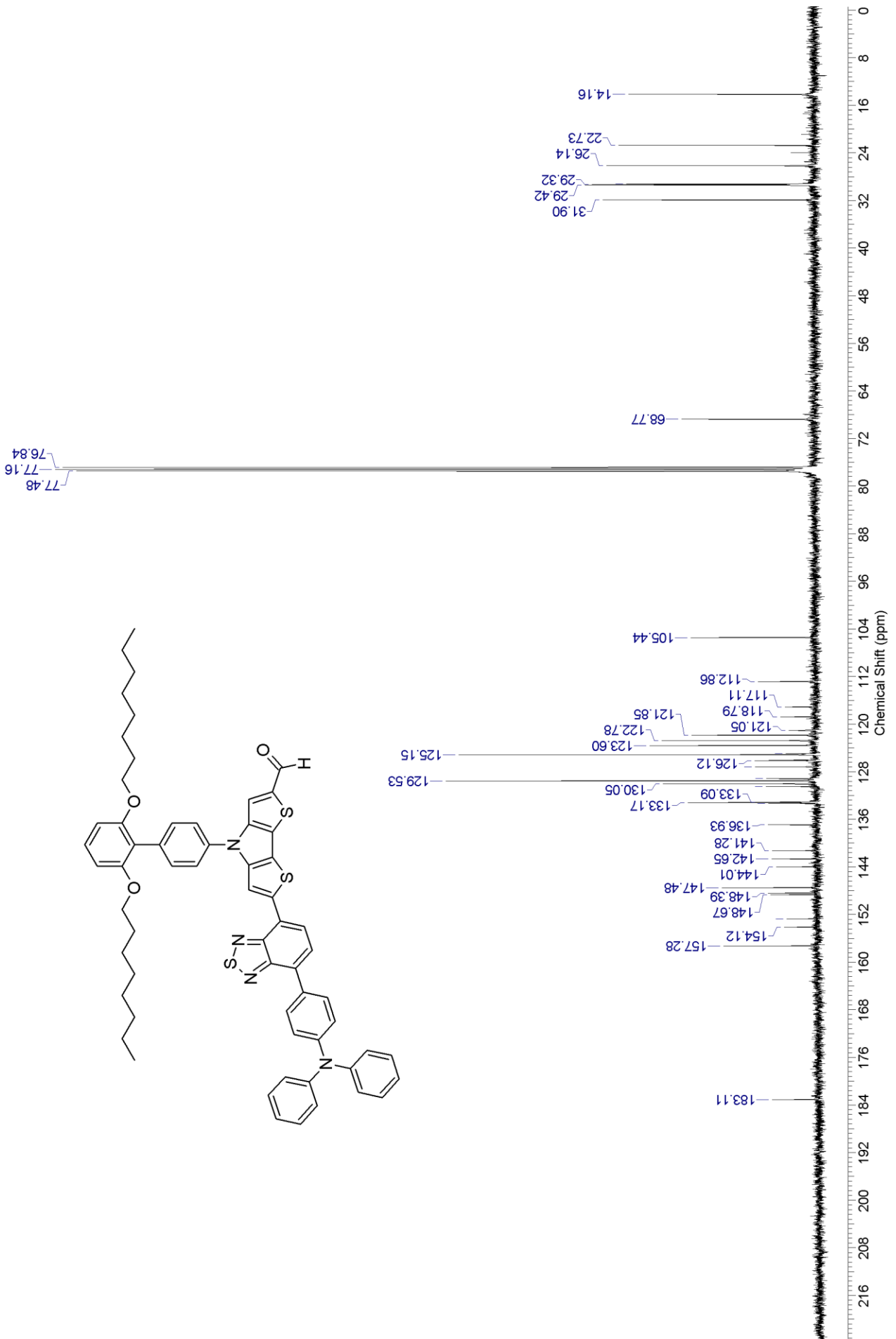
6. Copies of the NMR spectra of compounds 3, 4, 6, 8, BTD-DTP1-3.

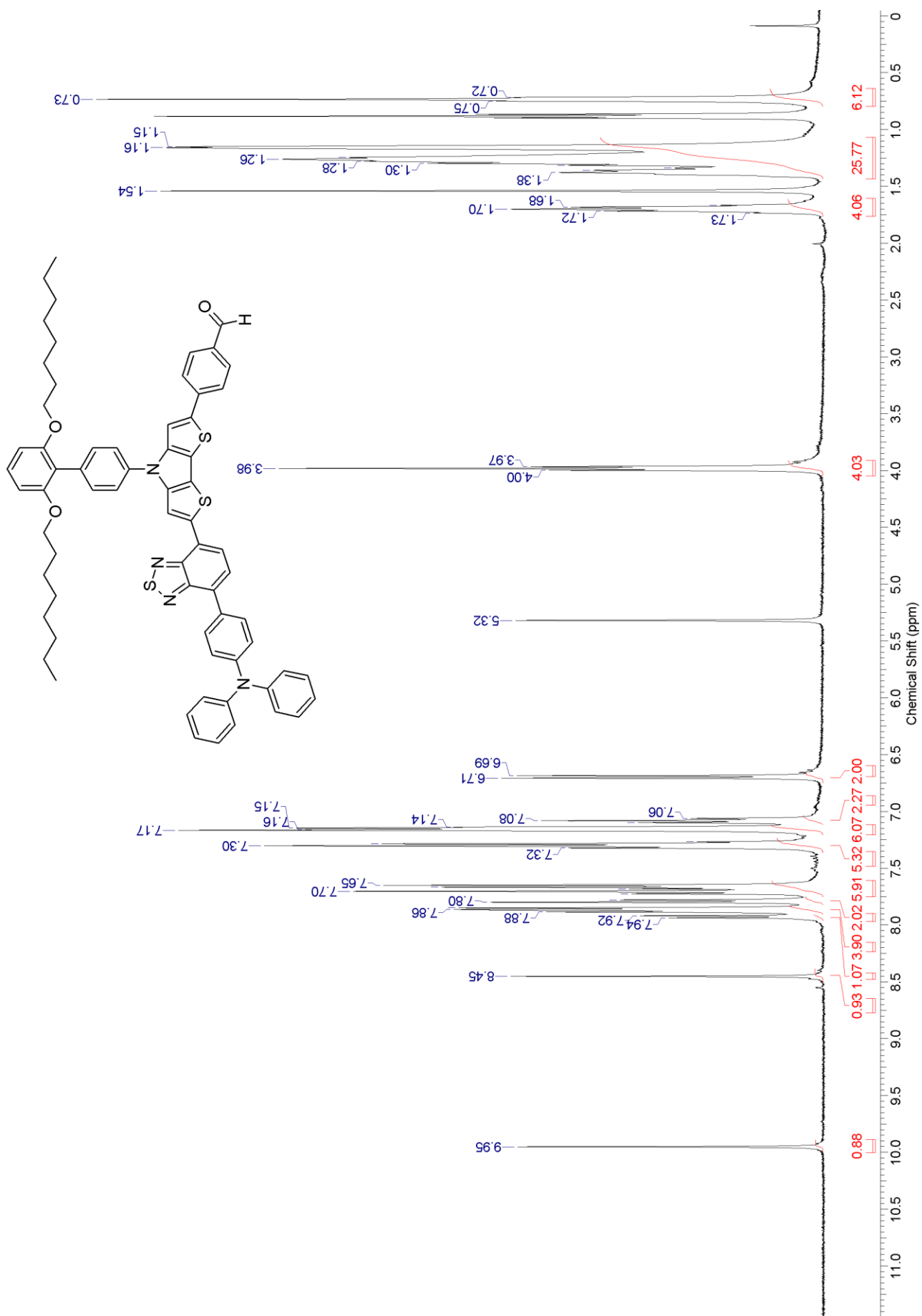


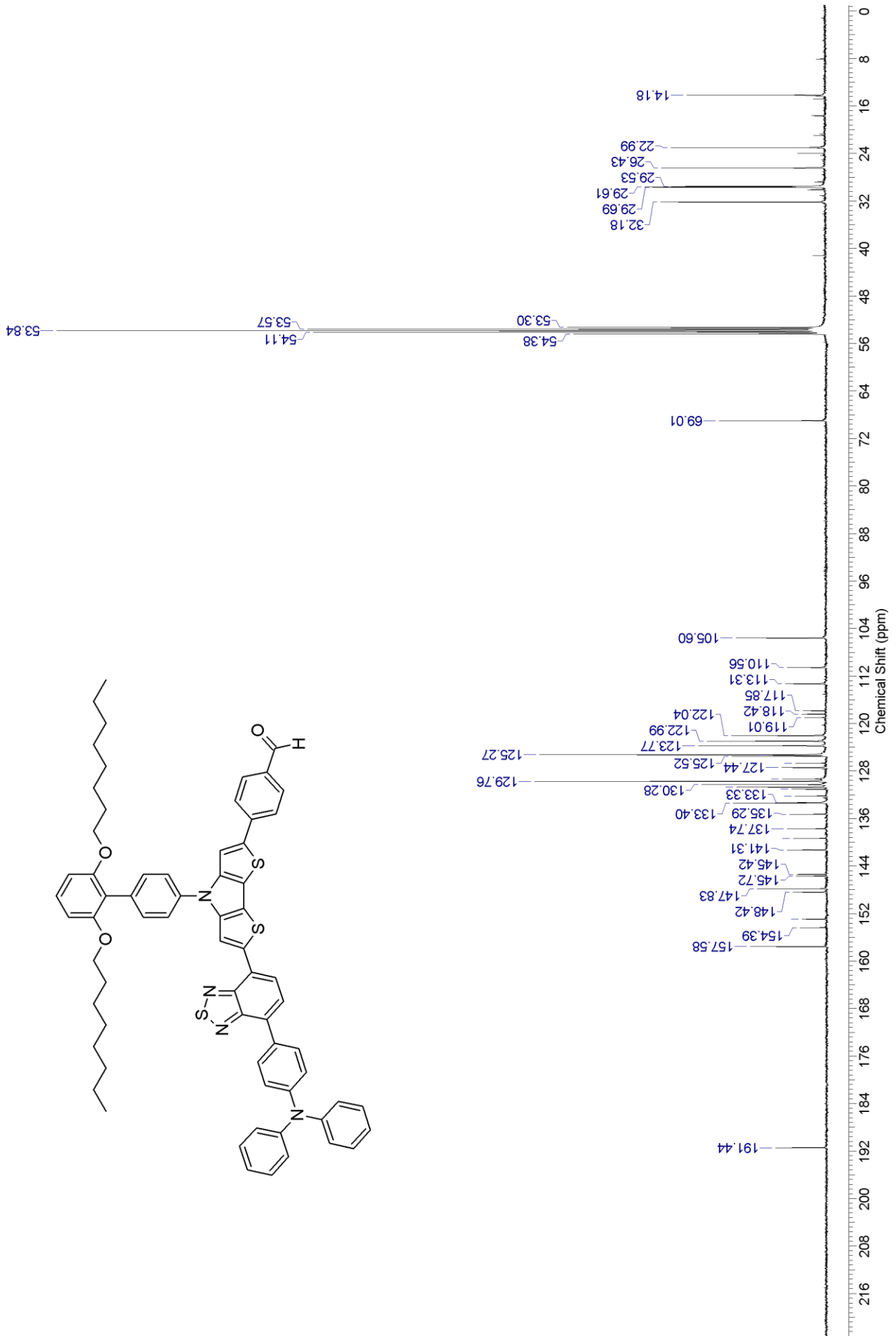


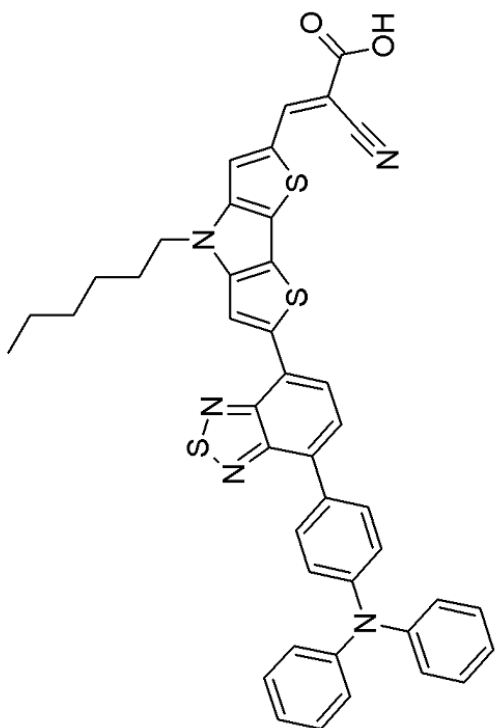
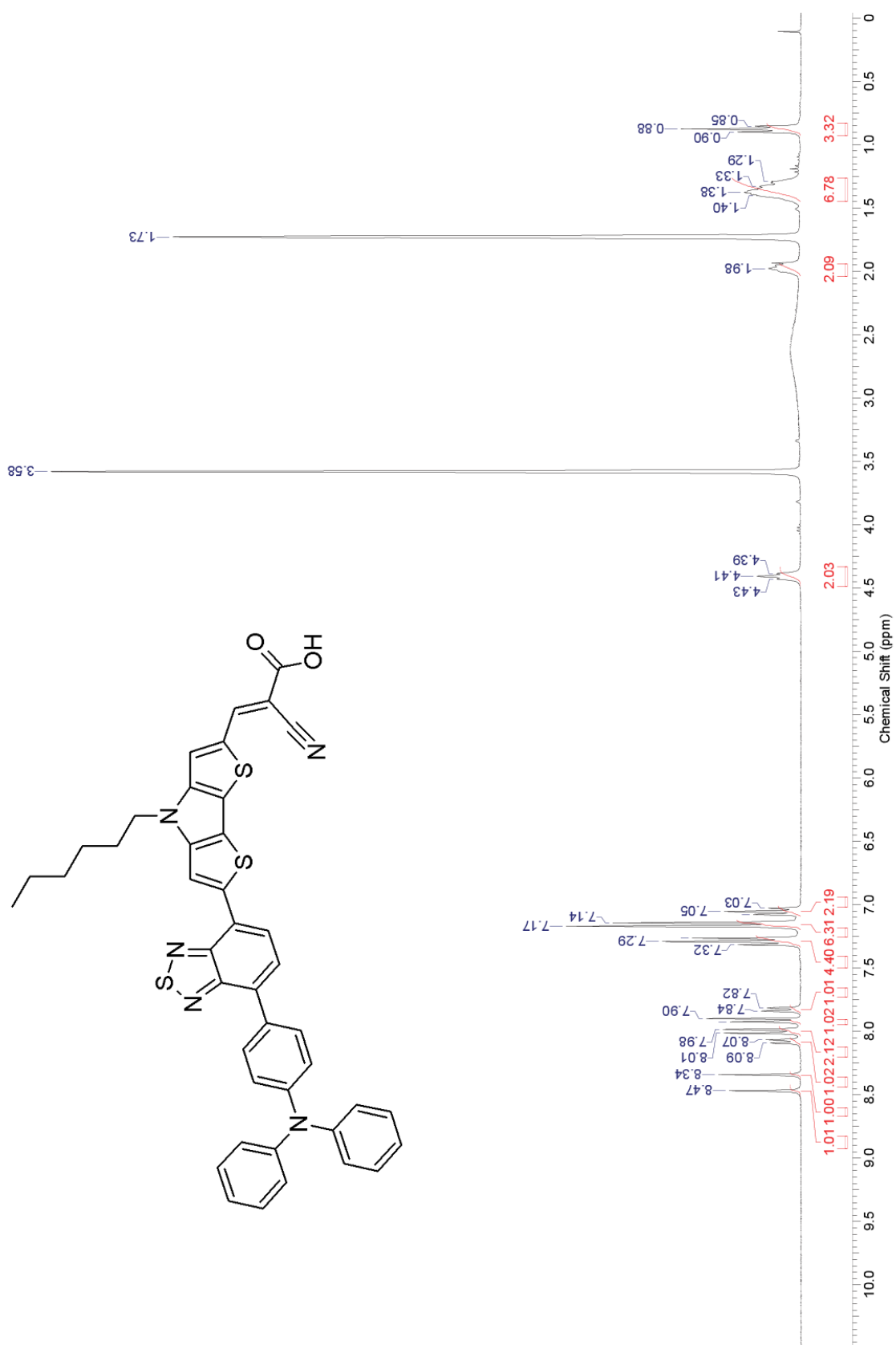


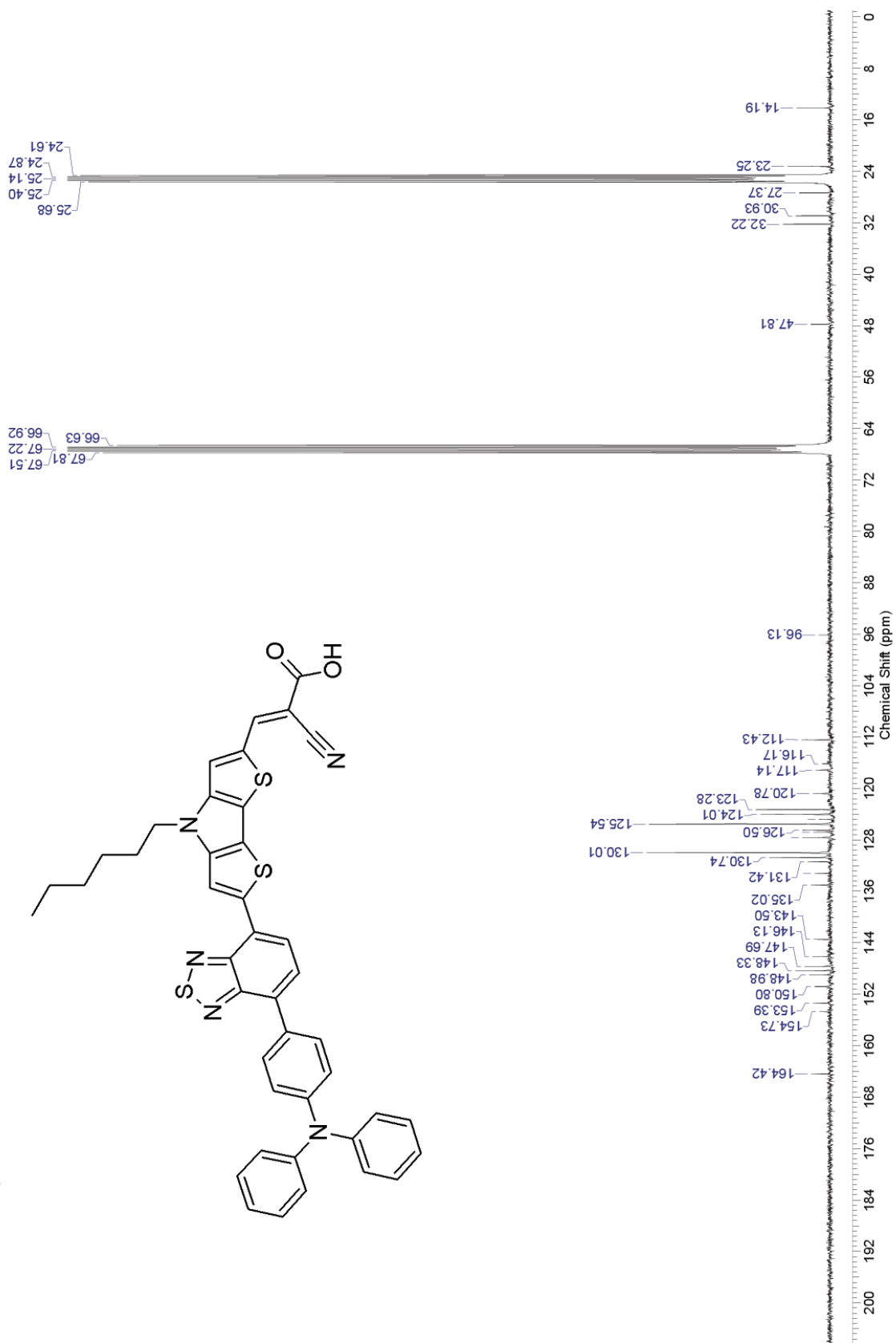


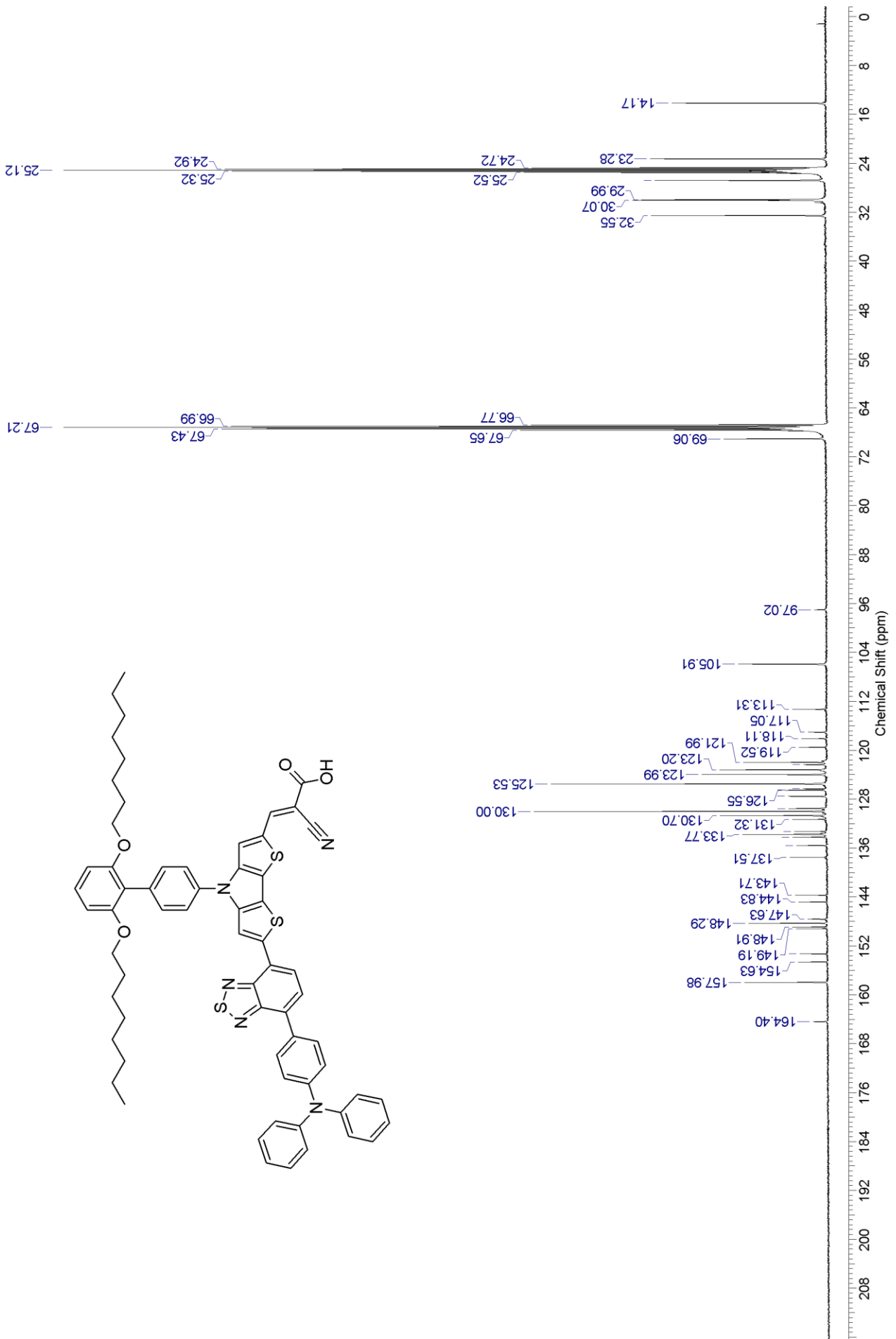


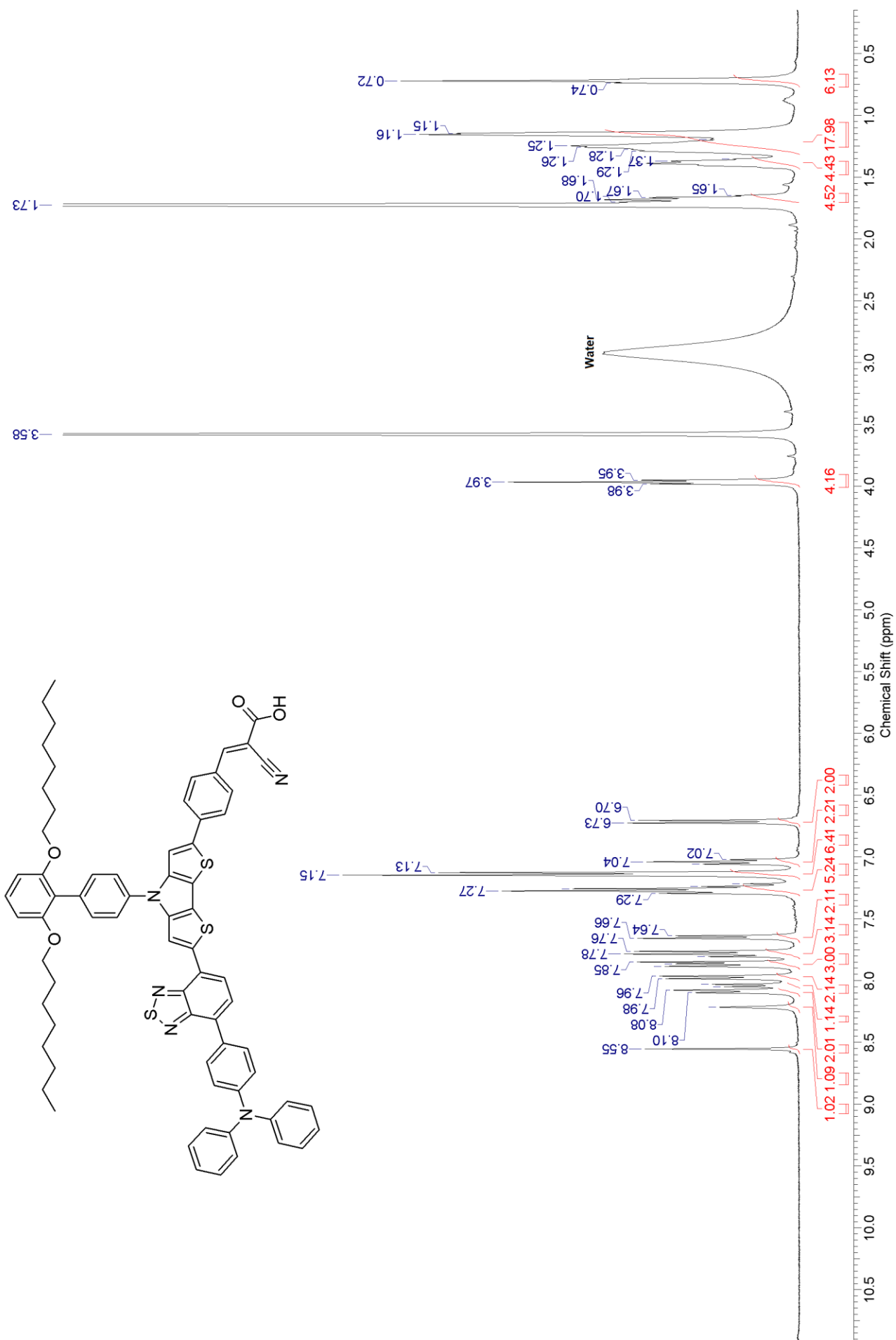


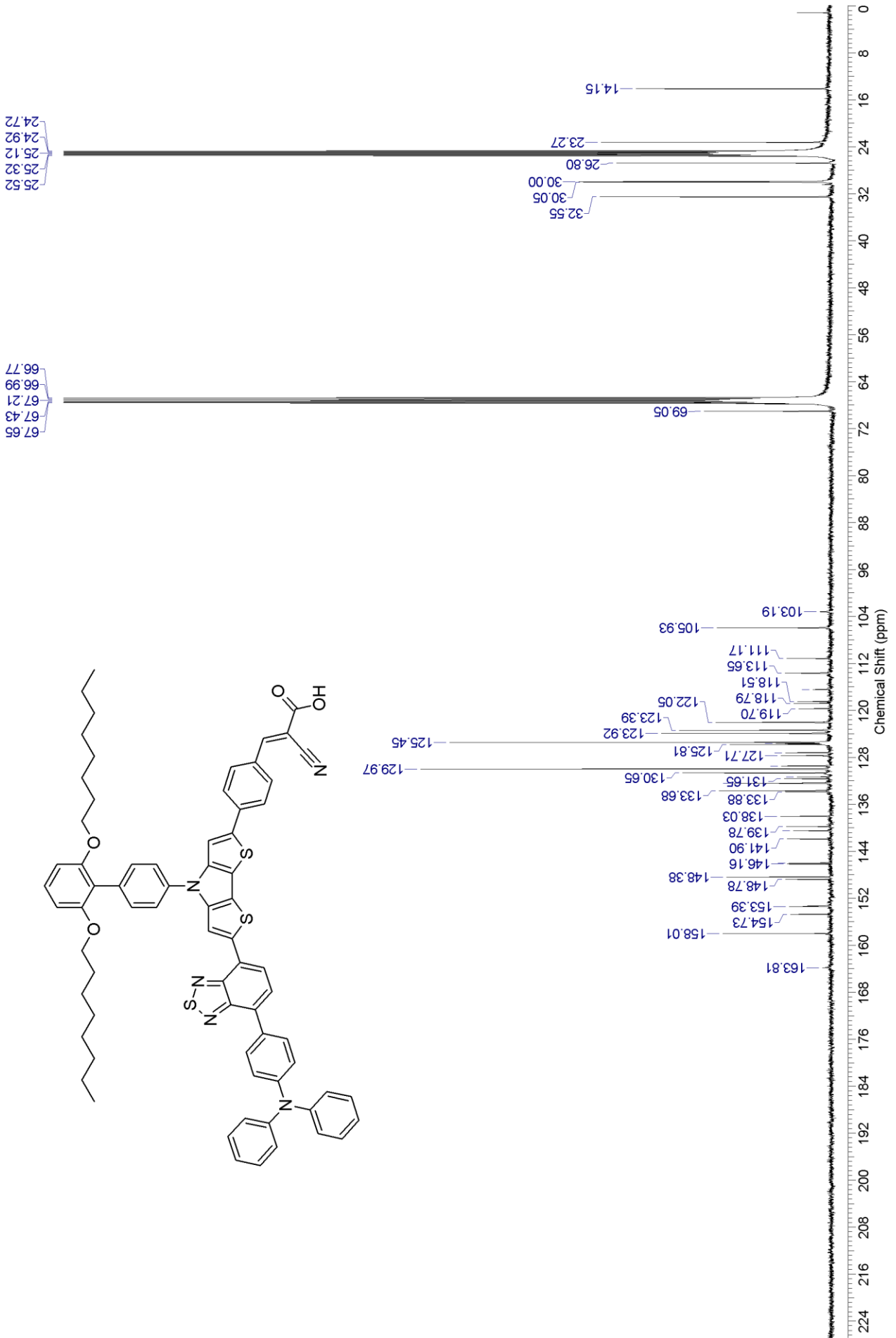












7. References

- 1 A. D. Becke, *Cit. J. Chem. Phys.*, 1993, **98**, 5648.
- 2 C. Lee, W. Yang and R. G. Parr, *Phys. Rev. B*, 1988, **37**, 785–789.
- 3 T. Yanai, D. P. Tew and N. C. Handy, *Chem. Phys. Lett.*, 2004, **393**, 51–57.
- 4 J. Tomasi, B. Mennucci and R. Cammi, *Chem. Rev.*, 2005, **105**, 2999–3094.
- 5 M. Paramasivam, R. K. Chitumalla, S. P. Singh, A. Islam, L. Han, V. Jayathirtha Rao and K. Bhanuprakash, *J. Phys. Chem. C*, 2015, **119**, 17053–17064.
- 6 M. Guo, R. He, Y. Dai, W. Shen, M. Li, C. Zhu and S. H. Lin, *J. Phys. Chem. C*, 2012, **116**, 9166–9179.
- 7 J. Wang, M. Li, D. Qi, W. Shen, R. He and S. H. Lin, *RSC Adv.*, 2014, **4**, 53927–53938.
- 8 M. J. Lundqvist, M. Nilsing, P. Persson and S. Lunell, *Int. J. Quantum Chem.*, 2006, **106**, 3214–3234.
- 9 A. Dessì, M. Calamante, A. Sinicropi, M. L. Parisi, L. Vesce, P. Mariani, B. Taheri, M. Ciocca, A. Di Carlo, L. Zani, A. Mordini and G. Reginato, *Sustain. Energy Fuels*, 2020, **4**, 2309–2321.
- 10 N. Cai, J. Zhang, M. Xu, M. Zhang and P. Wang, *Adv. Funct. Mater.*, 2013, **23**, 3539–3547.
- 11 W. Li, Q. Huang, Z. Mao, Q. Li, L. Jiang, Z. Xie, R. Xu, Z. Yang, J. Zhao, T. Yu, Y. Zhang, M. P. Aldred and Z. Chi, *Angew. Chemie Int. Ed.*, 2018, **57**, 12727–12732.
- 12 D. A. Chalkias, A. I. Laios, A. Petala and G. C. Papanicolaou, *J. Mater. Sci. Mater. Electron.*, 2018, **29**, 9621–9634.
- 13 S. Ito, M. K. Nazeeruddin, P. Liska, P. Comte, R. Charvet, P. Péchy, M. Jirousek, A. Kay, S. M. Zakeeruddin and M. Grätzel, *Prog. Photovoltaics Res. Appl.*, 2006, **14**, 589–601.